QUIET DRONES
Second International e-Symposium
on
UAV/UAS Noise
27th to 30th June 2022

Estimating Unmanned Aircraft Takeoff Noise Using Hover Measurement Data

Chris Cutler-Wood, US DOT Volpe Center: Chris.Cutler-Wood@dot.gov
Michael Barzach, US DOT Volpe Center: Michael.Barzach@dot.gov
Dr. Robert Downs, US DOT Volpe Center: Robert.Downs@dot.gov
Chris Hobbs, US FAA: Christopher.M.Hobbs@faa.gov
Susumu Shirayama, US FAA: Susumu.Shirayama@faa.gov

Summary

The Volpe Center, in support of FAA, has collected acoustic data from multiple unmanned aircraft over the last few years in a series of measurement campaigns. With this expanding dataset, it is now possible to estimate the noise produced by various types of flight operations and test the validity of those methods. Of particular interest in the context of environmental analyses is the noise produced during takeoff operations. This paper describes the process of using hover noise measurement data including directivity patterns to estimate the noise generated during takeoff procedures for an unmanned aircraft and presents a comparative analysis of the results and actual measurements.

1. UA Noise Measurement Campaigns

The FAA Office of Environment and Energy (AEE-100) sponsored two full-scale noise measurement campaigns with the Volpe Center's Environmental Measurement & Modelling Division (V-324) in 2021 to capture time-synchronized acoustics, tracking, and weather data to characterize noise emissions for various unmanned aircraft (UA). The first of the two campaigns took place in July 2021 at Causey Aviation Services (Causey), a small municipal airport near Liberty, NC. This location was chosen both for its relative remoteness (and the associated low ambient noise levels), and because it already served as a testing location for one of the UA operators whose platform was to be measured. The second measurement campaign was held at the Aviation Weather Research Facility (AWRF) on Joint Base Cape Cod (JBCC) in September 2021. This facility is a parcel of land operated by the Volpe Center and contains a large, grassy, runway-like area normally used for testing and validation of meteorological sensing and measurement equipment. Both campaigns used the same basic microphone array configuration pictured in Figure 1.

The microphone array comprised three distinct arrays: a linear array normal to the flight tracks of level overflights of the aircraft; a 50 ft. radius circular array whose center is below the aircraft hover position; and an elevated array consisting of 5 microphones up to 100 ft. above the ground to capture noise emitted from the plane of the rotors during both types of operations.

Microphones on the ground were inverted above ground boards. Microphones suspended from the crane were oriented vertically. All microphones used were pressure-field type and covered with windscreens. It should be noted that while the array configurations used at Causey and JBCC were the same, the orientation of East and West was flipped (the elevated and hover array mics were on the West side). For this paper, the Causey microphone positions will be referred to with the JBCC nomenclature; thus, the furthest mic position from the hovering UA was F45E at Causey, but it will be referred to as the F45W position in relation to Figure 1.

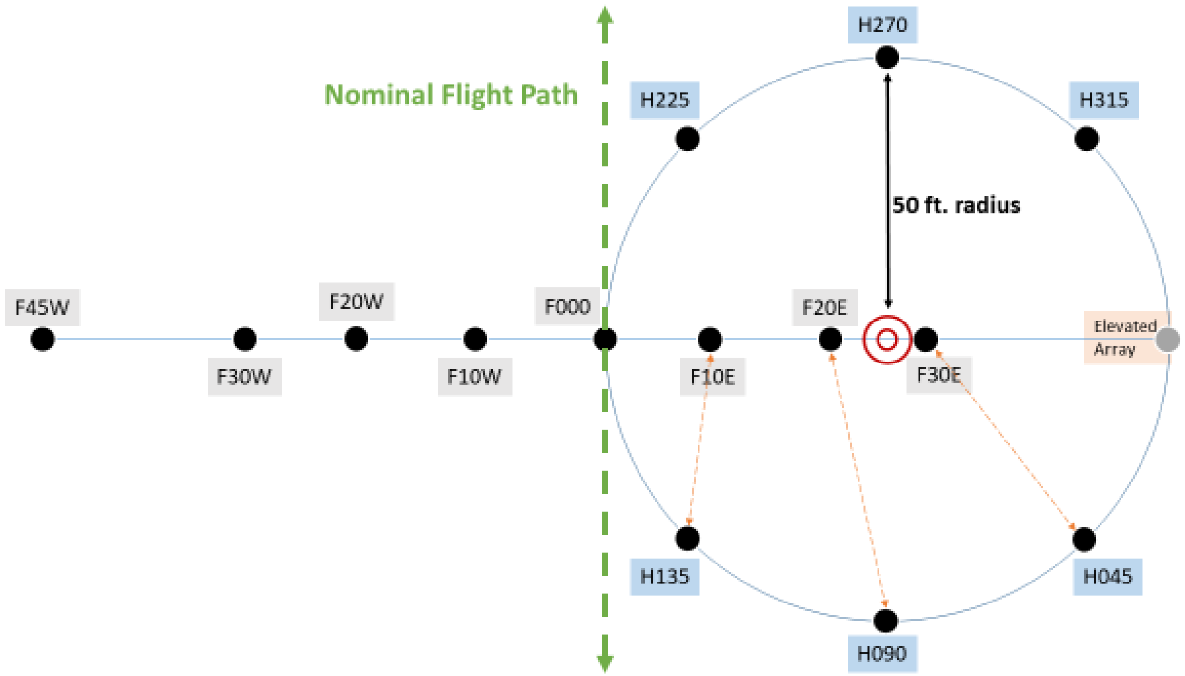

Figure 1. Microphone array configuration

1.1 Aircraft

This paper presents acoustic results for a pair of similar, six-rotor "hexcopters" measured during the two campaigns. The DJI M600 is a six rotor UA flown at JBCC and is similar to the Flytrex FTX-M600P flown at Causey. The following figures show these UA during their respective measurement campaigns and note their maximum takeoff weight. Aircraft were outfitted with a Volpe-designed differential GPS tracking device ("START" system) synchronized to the acoustic recording data. Flight log data were collected for each UA, including vehicle state, engine parameters, and orientation.

Figure 2. DJI M600 UA pictured at JBCC has a maximum takeoff weight of 33.3 pounds.

Figure 3. The Flytrex FTX-M600P flown at Causey has a maximum takeoff weight of 33.4 pounds.

1.2 Flight Test Points

During both measurement campaigns, the UA noise emissions were recorded when they were hovering at 50 ft. above the center of the circular array. The UA also performed vertical takeoffs starting near the center of the hover array. Local meteorological data were recorded from nearby weather stations to verify that the wind speed did not exceed 10 knots during measurement events. For the Causey measurement campaign, data were collected for all microphones during the test points. For the JBCC measurement campaign, all hover-, elevated-, and lateral-ground array microphones collected data, except for F10E, F20E, and F30E which were moved to positions on the circular array for the hover test points. Data for the DJI M600 and Flytrex M600P were collected at maximum takeoff weight performing these maneuvers, including a total of 6 events for each test point. All test points were not used in the analysis due to aircraft condition instability and/or position anomalies during the measured events. Table 1 shows a summary of the test points used for this analysis. The takeoff test points at Causey are not used here due to a pause during climb made by the Flytrex M600P as part of its programming. The takeoffs at JBCC were at constant speed for the length of the climb, though data from two takeoffs to an altitude of 100 ft. above the ground were trimmed to be the same height as the others to increase the number of test points used in the 50 ft. climb comparison. Recordings were made of the ambient noise levels throughout the days of testing. Ambient recordings were used to define the signal to noise ratio of the spectral time histories for each microphone recording. There was little to no evidence of noise levels above the ambient emitted from the UA below the 100 Hz one-third octave band. Accordingly, the spectra analysed in this paper comprise the 100 Hz through 10 kHz one-third octave bands. The 10 kHz one-third octave band is the upper frequency limit in the Advanced Acoustic Model (AAM), which is described in Section 2.

Table 1. Test Points used for Analysis

Test Point	Measurement Location	Aircraft & Configuration	Used For:
Hover	Causey	Flytrex M600P, Max Weight	FTRX Directional & Omnidirectional Spheres
Ambient	Causey	NA	Ambient for Causey
Takeoff	JBCC	DJI M600, Max Weight	Measured takeoff compared to Directional and Omnidirectional Spheres
Hover	JBCC	DJI M600, Max Weight	M600M Omnidirectional Sphere
Ambient	JBCC	NA	Ambient for JBCC

2. Noise Hemisphere Creation

The AAM is used here to estimate sound levels from vehicles performing typical operations whose noise emissions have been characterized in the form of noise sphere files (Page, 2012). Noise sphere files represent the noise emissions from a vehicle in a particular orientation and for a operating state. Spherical coordinates are used to define the vehicle orientation. One-third octave band spectral noise levels were used for this analysis. The noise sphere spectra represent the free field emissions in each direction, starting at a fixed radius of 100 ft with no atmospheric absorption. This allows the noise sphere files to be used to model different meteorological conditions.

2.1 Omnidirectional Sphere Creation

Hover test point data were nominally collected for 30 seconds during which the UA was in a stable flight condition. Data were analysed to create one-third octave band time histories. Spectral time history and synchronized tracking data were reviewed to confirm the stability of the aircraft position and identify any potential intrusive or contaminating noise.

The L_{eq} for each one-third octave band was calculated from the spectral time history for each microphone. The actual distance between the UA and microphone was used to normalize the distance of each L_{eq} spectrum to the same distance using spherical spreading. An average spectrum was calculated from the normalized spectra for each UA event hovering at 50 ft to produce an average one-third octave band spectrum from each of the 6 recordings of the UA.

Any average spectrum identified as an outlier was removed from further processing. The remaining spectral averages were averaged together using simple arithmetic mean to produce a spectrum representing the UA hovering at 50 ft.

The average spectrum was used to create an omnidirectional noise sphere for use in the AAM. To make the noise sphere from the average spectrum of the UA hovering at 50 ft., the atmospheric absorption had to be removed using the normalized distance and average meteorological data. The levels were then corrected for the difference between the normalized distances of the spectra to the radius of the sphere (100 ft.) using spherical spreading. Finally, 6 dB was subtracted dB from each one-third octave band level in the average spectrum to account for ground effect.

2.2 Directional Hover Sphere Creation

In order to estimate any directionality of the noise emissions from the hovering UA, another approach to sphere making was undertaken. By considering the noise emissions from hovering UA to be axisymmetric, the spectrum recorded at each ground mic can be used to represent the noise emissions from any point about the vehicle at the same angle from the vehicle's vertical axis. In terms of noise spheres, this is equivalent to replicating the same spectrum at all longitudes for the same latitude on a sphere whose axis is vertical. Because the noise spheres used by AAM have their axis horizontally oriented, a coordinate transformation had to be performed before creating the sphere. While noise levels at frequencies corresponding to the blade passage frequencies are not necessarily constant due to destructive and constructive interference of the frequencies emitted from each of the motors, one-third octave band spectra and analysis that relies on the average sound level should reduce the influence of those interference effects.

Because the spectra from each microphone have been corrected for the effects of propagation to a distance of the sphere radius and the atmospheric absorption was added back into the recorded levels, they can be considered as depropagated noise levels. Furthermore, the noise sphere format for AAM requires noise levels on a fixed grid of points at even intervals in (Phi, Theta) coordinates, as shown in Figure 4. In order to create a regular grid of noise levels from the data from the ground microphone positions, the grid data were estimated using a Laplacian interpolation in the Acoustic Repropagation Technique (ART) program (Page, 2004). The interpolation procedure uses nearest-neighbor data points on the sphere's surface to estimate the levels for each grid point. This results in estimated levels at grid points on the sphere representative of higher elevation angles than the furthest away microphones.

Consider the contours of the 1 kHz one-third octave band levels on the directional sphere created from ground microphone recordings during the Flytrex M600P hovering at 50 ft. in Figure 4. The noise received at each microphone will have been emitted from a direction represented by a point on the sphere. Assuming symmetry about the vertical axis of the UA for noise emissions, the depropagated noise received at a microphone can be assigned to a ring of coordinates with the same angle relative to the UA's vertical axis. Depropagated spectra from all ground microphone recordings will be used in the ART program to find the spectra on a regular grid. Note the black lines in the Figure 4 show the rings on the sphere (one for each microphone position). The abundance of rings crossing 0 degree phi and 45 and 135 degree theta angles represent the hover mics all being near the same position relative to the vehicle during the hover recordings. The directionality of the 1 kHz one-third octave band noise emissions is evident in the decrease in level from underneath the UA (0° Phi, 90° Theta) towards the plane of the rotor (90° Phi). It is understood that broadband noise from rotors should follow this pattern (George, 1984).

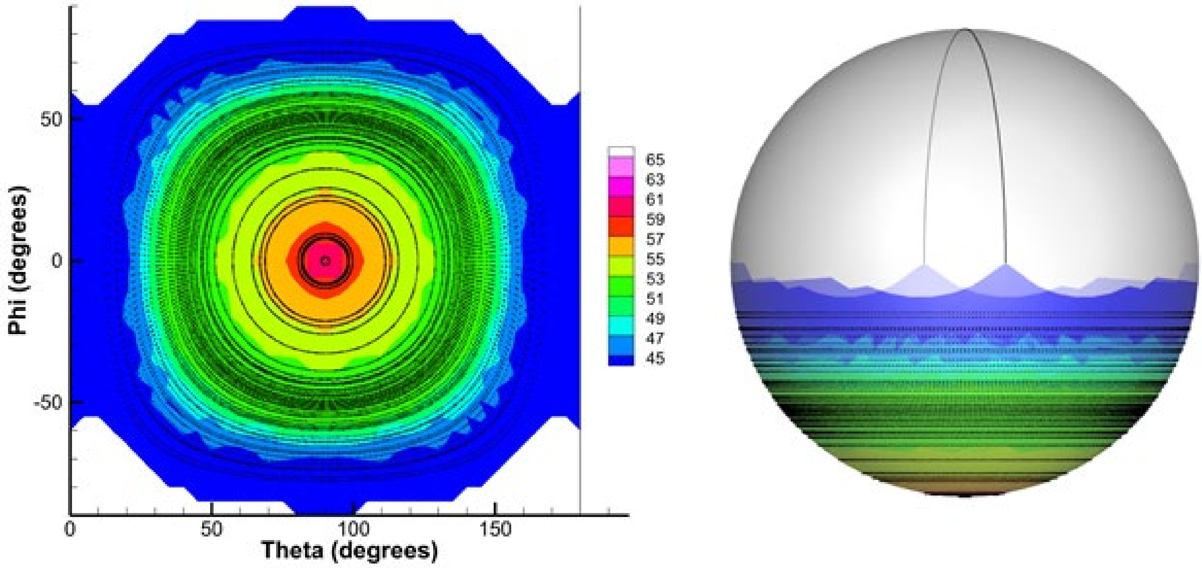

Figure 4. Contours of 1 kHz one-third octave band levels on two views of the directional noise sphere with decibel levels noted in legend and microphone data input represented by dashed black lines assuming axisymmetric noise emissions.

The result of this reduction and processing was noise spheres containing the average one-third octave band spectra of each UA hovering at 50 ft. The aircraft are listed in Table 2, along with their configurations and the name of the noise sphere ".NC" file.

Table 2. Omnidirectional Noise Spheres Created from JBCC and Causey Measurements

UA Model	Test Point	Configuration	Sphere Name (*.NC)	Directionality
DJI M600	50 ft. Hover	Max. Weight (33.3 lbs)	M600M	**Omni**
Flytrex M600P	50 ft. Hover	Max. Weight (33.4 lbs)	FTRXM	**Omni**
Flytrex M600P	50 ft. Hover	Max. Weight (33.4 lbs)	FTRXD	**Directional**

A comparison of the two spectra used to make the omnidirectional hover spheres is shown in Figure 5. The behaviour of the broad band portion of the spectra is similar in amplitude and shape. The bands at the blade passage frequencies do show a difference. The DJI M600's blade passage frequency noise is shared between the 100 and 125 Hz one-third octave bands. It is important to understand that the spectra shown in Figure 5 have no atmospheric absorption and represent the levels spherical spread to 100 ft. The two spectra represent the average levels measured only on the hover ring microphones while the vehicles were hovering at 50 ft. above the center of the ring, as detailed above.

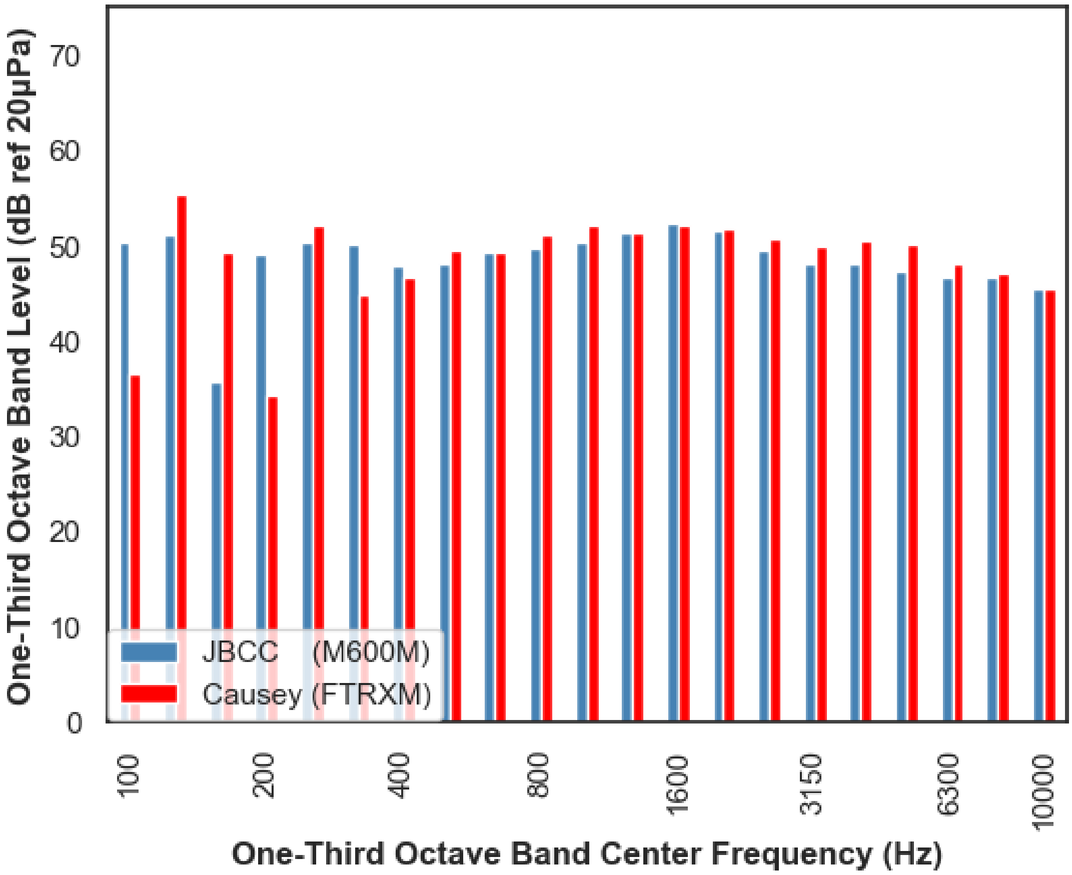

Figure 5. Comparison of average spectra of DJI M600 and Flytrex M600P from 50 ft. hover condition.

3. Analysis

The analysis consisted of comparisons between the noise sphere and measured acoustic data using AAM to model the noise for the as-flown test points. The run-specific weather conditions and associated atmospheric absorption effects were used with each noise sphere to predict noise levels at microphone locations.

3.1 Estimating Hover Noise Levels Using Omnidirectional Hover Noise Hemisphere

The first analysis used the omnidirectional hover noise sphere in conjunction with the tracking data from the 50 ft. hover events to estimate noise levels at the hover ring microphone locations originally used to create the noise spheres. Although the noise spheres are an average of noise from similar hover events, this comparison was expected to produce noise levels similar to the actual measured data for each of the hover events included in the noise hemisphere. A sample comparison is shown in Figure 6 for one run at the 50 ft. hover test point at JBCC.

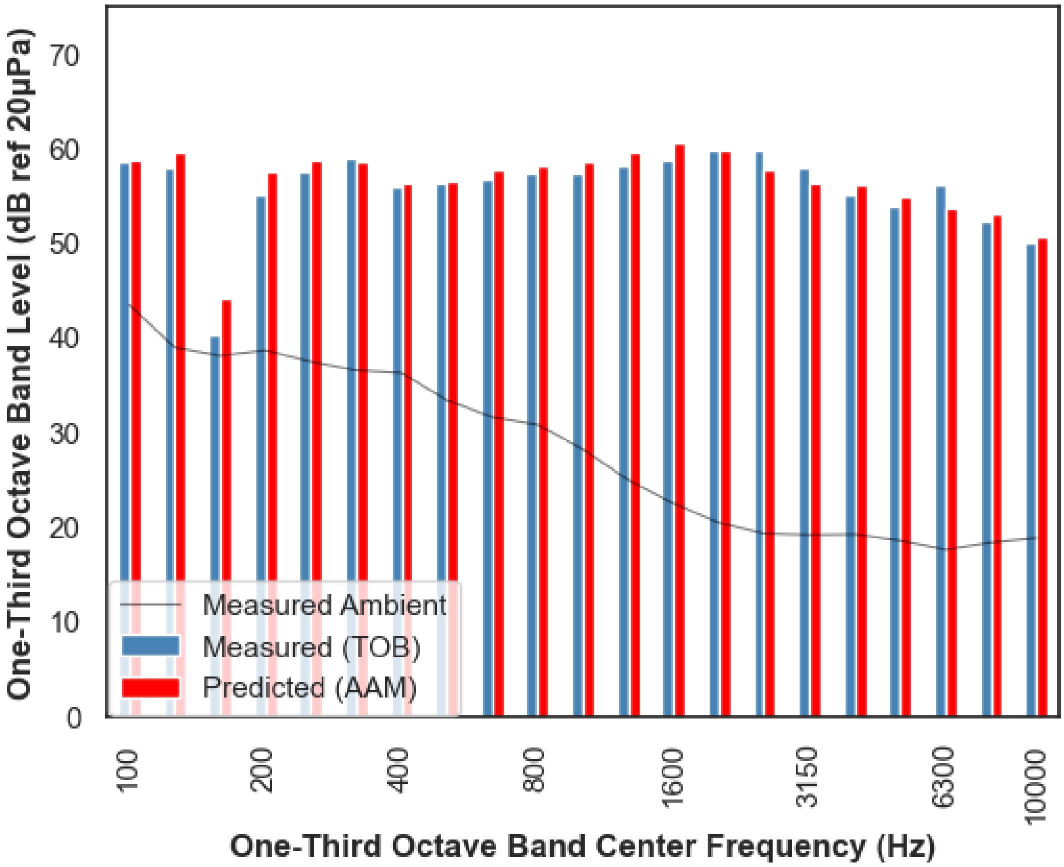

Figure 6. Measured and estimated levels of M600M at hover ring microphone H270.

Overall, the results follow the expected outcome. Generally, the estimated one-third octave band levels are in agreement with the actual measured levels for the 50 ft. hover events for all aircraft, especially in the broadband spectra (around 1 kHz). There was some discrepancy in the lower frequencies close to the blade passage frequency of each aircraft (generally the 100 Hz or 125 Hz one-third octave bands), which could potentially be attributed to band-sharing or slight variations in blade passage frequency that push the acoustic energy into neighbouring one-third octave bands.

3.2 Estimating Lateral Noise Levels Using Omnidirectional Hover Noise Hemisphere

The second comparison used the omnidirectional hover noise sphere to predict the noise levels at the lateral ground microphone locations on the linear microphone array extending outside the hover array. Note these microphone data were not used to create the omnidirectional noise sphere. It was expected that the broadband noise levels at these lateral microphone positions would be over-predicted (that is, the estimated noise levels would be higher than the actual measured noise levels) due to the observed directional nature of the broadband noise shown in Figure 4. A comparison of the difference in broadband noise at a lateral microphone located 150 ft. to the side of the hover point is shown in Figure 7. The difference in the levels 400 to 3150 Hz one-third octave bands is evident.

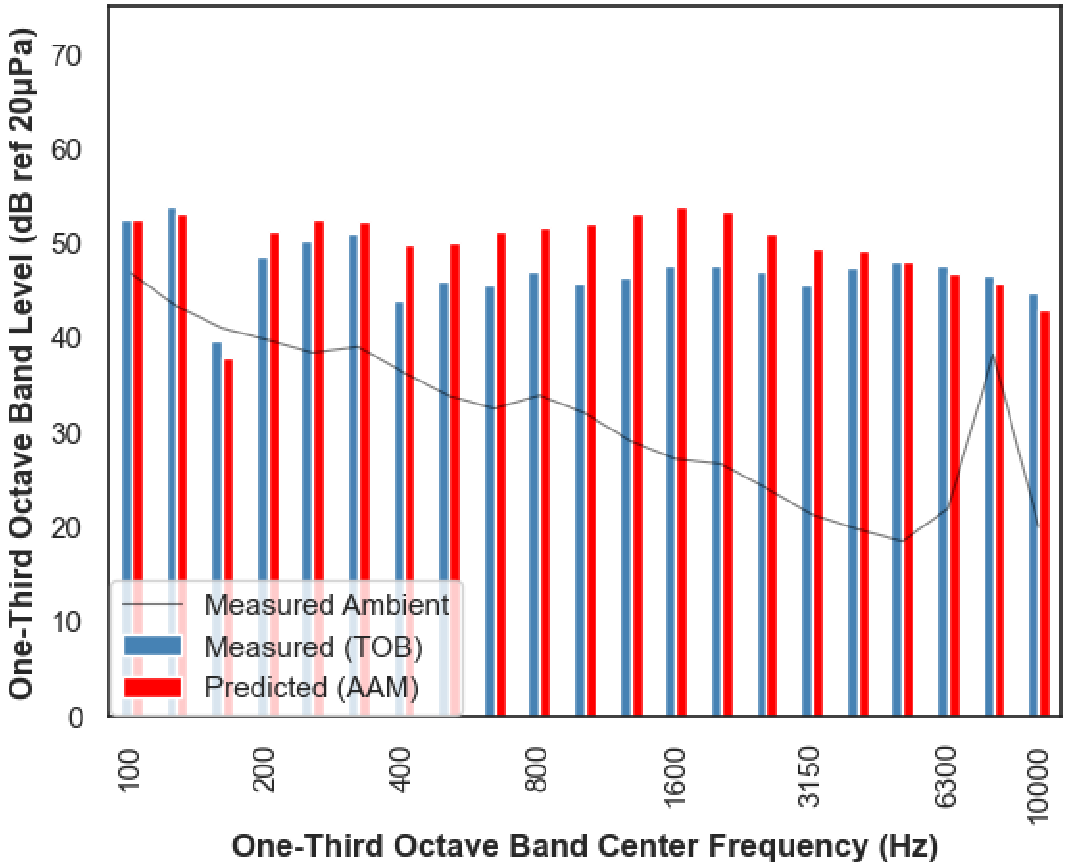

Figure 7. Measured and estimated levels of M600M at lateral microphone F45W.

3.3 Estimating Lateral Noise Levels Using Directional Hover Noise Hemisphere

To investigate the relative accuracy of hover noise predictions using the directional hover noise sphere, the initial comparison was replicated using the directional hover noise sphere. The results show that the directional noise sphere more accurately predicts noise levels at the lateral microphone positions, when compared to the noise levels predicted by the omnidirectional noise sphere. Figure 8 shows the predicted versus measured noise levels at the Causey F45W lateral microphone position for the FTRXD noise sphere during a 50 ft. hover event. Compared to Figure 7, the prediction of one-third octave band noise levels, especially broadband noise around 1 kHz, is much more in line with the actual measured noise levels for the hover event.

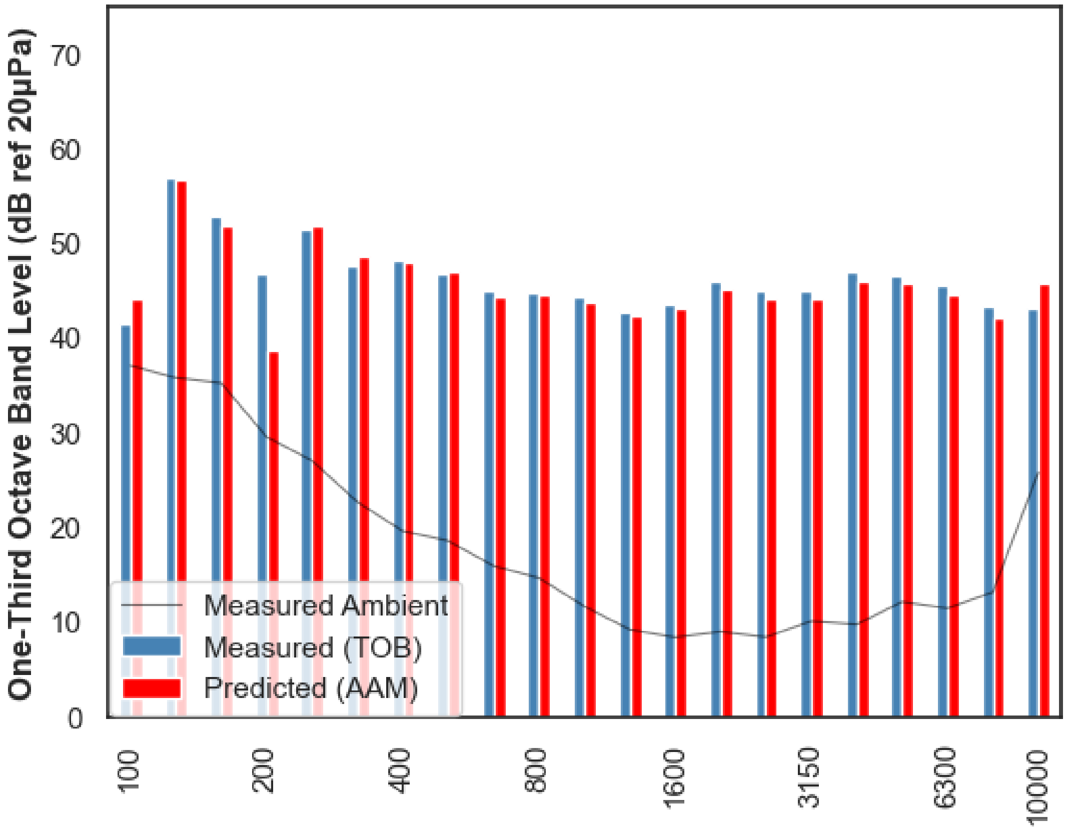

Figure 8. Measured and estimated levels of FTRXD at lateral microphone F45W during Causey measurements.

3.4 Estimating Takeoff Noise Levels Using Hover Noise Sphere

The final comparison used the spheres created above with takeoff event trajectory data. Five takeoff events recorded at JBCC were used for this comparison. Four events were takeoffs to approximately 50 ft. before transitioning to horizontal flight, while one event was a takeoff to 100 ft. before transitioning to horizontal flight. All five events behaved similarly near the ground, with the initial ascent being a slow climb to about 6 ft. above the ground followed by a constant speed ascent to the transition altitude. Figure 9 shows a plot of the takeoff event to 100 ft. before transitioning to horizontal flight by the DJI M600 at JBCC. The elevated microphone array mentioned in Figure 1 is shown to scale. The altitude profile is shown in the following figure with the initial change in climb rate around 6 ft. above ground level.

In order to isolate just the climb portion of the takeoff events, the trajectories of all five events were trimmed to start when the aircraft reached 6 ft. in altitude and end at 47 ft. The 47 ft. upper altitude was used because it was the lowest common top altitude of the 5 events. The average position was used for the horizontal position during the climb events. This was done to smooth out the tracking data and more accurately represent how the noise spheres were created, relative to the horizon. All three noise spheres were used to model a takeoff event in AAM. The estimated arrival time of the sound at each of the microphone locations was used to calculate the sound exposure level (L_{AE}) of the A-weighted time history for each microphone. This is not the same as the total event L_{AE} which would include the transition noise between hover and vertical ascent, and initial motor start up. The objective of this exercise was to have a consistent set of trajectories and recordings to compare the effects of directivity in levels recorded as a function of distance along the ground from a takeoff event.

Recall that the recordings at JBCC were of the DJI M600 UA taking off at maximum weight. The comparisons with the Flytrex noise spheres are being done because the directional noise sphere could only be made with the data captured during the Causey measurement campaign due to the microphone array configuration during the hover events. The takeoff events of the Flytrex M600P could not be used for the comparison because of a significant pause at around 30 ft. above ground level in the takeoff ascent.

Because the Flytrex M600P and DJI M600 platforms are similar in configuration and weight, along with the spectral comparison shown above, it is reasonable to expect the DJI M600 to have a similar broadband directivity pattern as the Flytrex M600P. Therefore, it is justifiable to use the modelling substitute for the takeoff recordings at JBCC below.

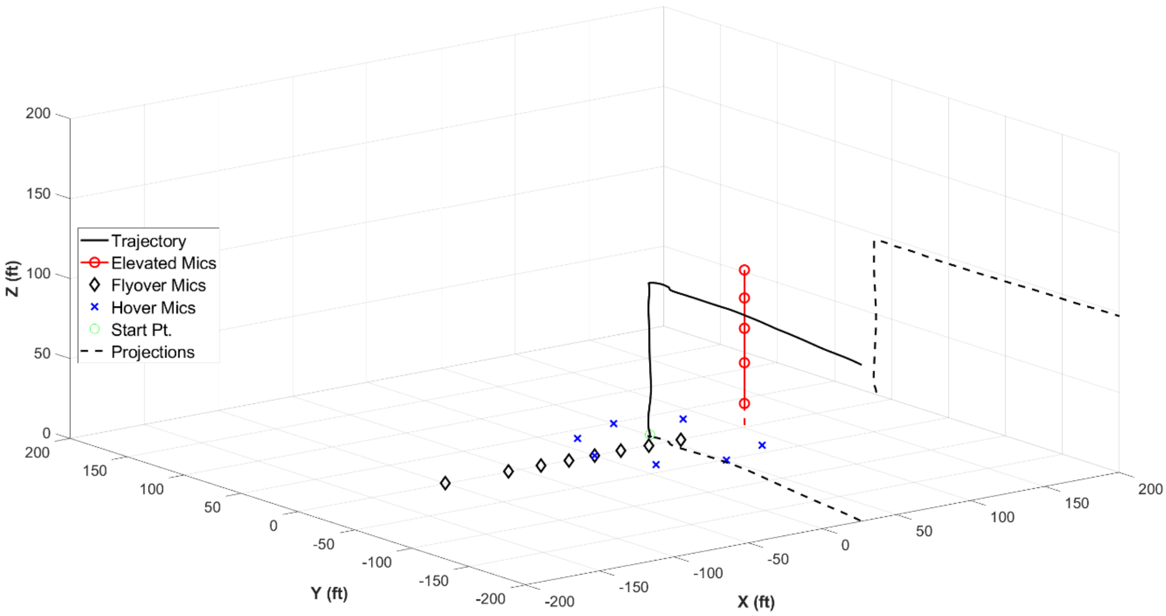

Figure 9. Takeoff event of DJI M600 at JBCC with transition to horizontal flight at 100 ft. above ground level.

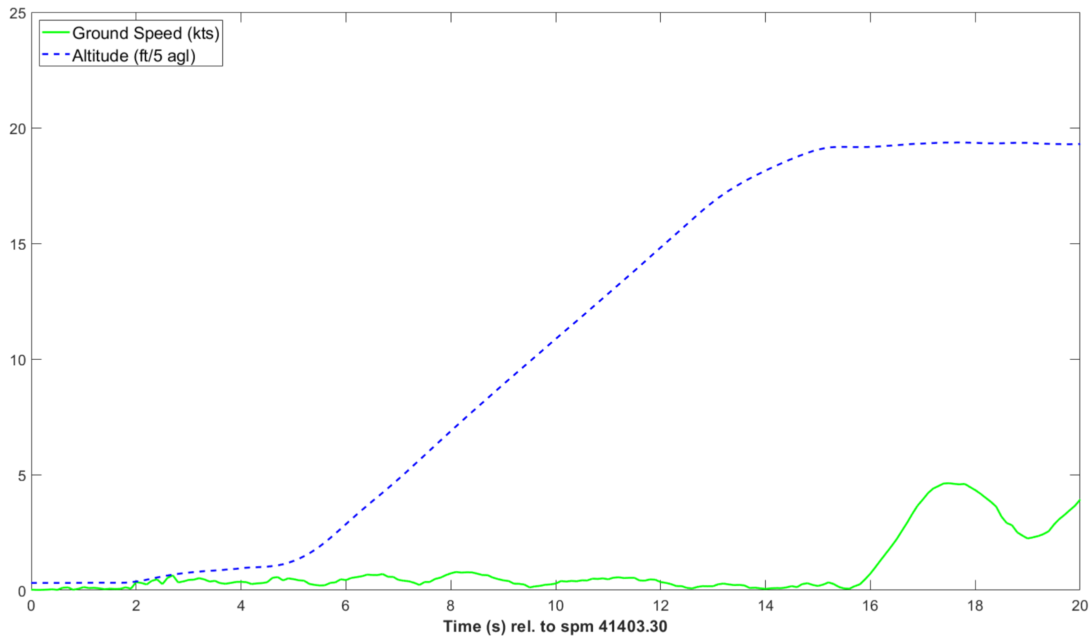

Figure 10. Altitude profile of takeoff event to 100 ft. transition shown with ground speed.

The results of modelling the trimmed trajectories of the five event and calculating the received noise at each microphone are listed in Table 3.

Table 3. Measured and Modelled L_{AE} for Trimmed Takeoffs at JBCC

Source	Lateral Distance (ft.)	7	14	33	50	67	86	108	150
	Event\Mic	**F30E**	**F20E**	**F10E**	**F000**	**F10W**	**F20W**	**F30W**	**F45W**
Measured	RUN0064	87.8	88.3	83.4	79.8	76.0	72.2	69.1	63.3
	RUN0072	90.0	92.1	84.6	80.4	76.9	73.2	70.0	64.3
	RUN0074	90.6	90.0	83.6	80.0	76.7	73.1	69.6	64.5
	RUN0081	88.3	86.6	81.0	77.6	74.5	71.5	69.1	64.0
	RUN0089	91.6	89.9	83.1	79.3	75.9	72.0	69.2	64.2
	RUN0100	87.8	88.3	83.4	79.8	76.0	72.2	69.1	63.3
Modelled	RUN0064_FTRXD	85.9	85.4	80.1	76.7	73.3	70.2	68.0	63.8
	RUN0064_FTRXM	85.2	84.8	81.6	79.0	76.8	74.9	73.0	70.1
	RUN0064_M600M	84.4	83.9	80.7	78.1	76.0	74.0	72.2	69.3
	RUN0072_FTRXD	86.7	88.2	83.1	78.3	75.7	72.9	69.5	64.9
	RUN0072_FTRXM	85.9	86.9	83.3	80.5	78.2	76.1	74.2	71.2
	RUN0072_M600M	85.0	86.0	82.5	79.6	77.3	75.3	73.4	70.4
	RUN0074_FTRXD	87.0	86.6	81.1	77.1	74.3	71.5	68.5	64.1
	RUN0074_FTRXM	85.9	85.8	82.2	79.5	77.3	75.3	73.4	70.5
	RUN0074_M600M	85.1	84.9	81.4	78.7	76.4	74.5	72.6	69.7
	RUN0081_FTRXD	86.5	85.9	80.8	77.5	74.5	71.4	69.0	64.8
	RUN0081_FTRXM	85.8	85.2	82.1	79.6	77.5	75.6	73.8	70.9
	RUN0081_M600M	85.0	84.4	81.3	78.8	76.7	74.8	72.9	70.1

By calculating the difference levels between each of the estimates from modelling the noise spheres in AAM and deriving the average of the difference levels, the improvement in estimating lateral noise during the ascent portion of a takeoff operation using the noise sphere with directivity is apparent, as shown in Table 4.

Table 4. Difference Levels of Modelled and Measured L_{AE} for Takeoffs Events at JBCC

Lateral Distance (ft.)	7	14	33	50	67	86	108	150
RUN_Sphere\Mic	**F30E**	**F20E**	**F10E**	**F000**	**F10W**	**F20W**	**F30W**	**F45W**
RUN0064_FTRXD	-2	-3	-3	-3	-3	-2	-1	1
RUN0072_FTRXD	-3	-4	-2	-2	-1	0	-1	1
RUN0074_FTRXD	-4	-3	-3	-3	-2	-2	-1	0
RUN0081_FTRXD	-2	-1	0	0	0	0	0	1
RUN0089_FTRXD	-4	-3	-2	-3	-2	-1	-1	-1
FTRXD-Ave-Diff	**-3**	**-3**	**-2**	**-2**	**-2**	**-1**	**-1**	**0**
RUN0064_FTRXM	-3	-4	-2	-1	1	3	4	7
RUN0072_FTRXM	-4	-5	-1	0	1	3	4	7
RUN0074_FTRXM	-6	-5	-2	-1	0	1	3	5
RUN0081_FTRXM	-3	-1	1	2	3	4	5	7
RUN0089_FTRXM	-5	-4	-1	0	1	3	4	6
FTRXM-Ave-Diff	**-4**	**-4**	**-1**	**0**	**1**	**3**	**4**	**6**
RUN0064_M600M	-3	-4	-3	-2	0	2	3	6
RUN0072_M600M	-5	-6	-2	-1	0	2	3	6
RUN0074_M600M	-6	-5	-2	-1	0	1	3	5
RUN0081_M600M	-3	-2	0	1	2	3	4	6
RUN0089_M600M	-6	-5	-2	-1	0	2	3	5
M600M-Ave-Diff	**-5**	**-5**	**-2**	**-1**	**1**	**2**	**3**	**6**

As expected, and similar to the hover event comparisons, the omnidirectional hover spheres overestimated takeoff noise at the far lateral microphone positions when used to predict takeoff noise levels. There was generally good agreement between the L_{AE} values determined using the Causey and JBCC omnidirectional spheres, despite being from different measurement campaigns. Both the omnidirectional and directional noise spheres underestimated the noise levels underneath the vehicle during takeoff. The predictions using the omnidirectional noise sphere generally over predicted the noise levels at the furthest lateral mic by 6 dB.

4. Conclusion

Despite their small size, the UA studied here show directivity in their broadband noise emissions. Because of this directivity, using the noise levels from 45 degrees below the UA as an estimate for noise emissions in all directions may result in an overestimate of takeoff noise at further lateral positions. Estimation of takeoff sound exposure levels is more accurate using noise spheres which include the directionality of the UA noise, even if the directionality is taken from a different flight condition, such as a hover.

It is worth noting that the L_{AE} values predicted using directional noise spheres more closely match actual measured values at both hover and lateral microphone positions. The predicted noise levels using the directional hover sphere accurately estimate the takeoff noise levels (L_{AE}) at the lateral microphone positions within at least 1 dB. That being said, the predicted noise levels using the directional noise sphere still underestimate the noise generated underneath the aircraft (though, to a smaller degree than the omnidirectional noise sphere predictions).

References

Page, J.A., Wilmer, C., Schultz, T., Plotkin, K.J., Czech, J., (2010) *Advanced Acoustic Model Technical Reference and User Manual*, SERDP Project WR-1304, Wyle Laboratories Research Report No. WR 08-12, Wyle Laboratories, Inc., Arlington, VA., Sept. Available from: http:// www.serdp.org/Program-Areas/Weapons-Systems-and-Platforms/Noise-and-Emissions/Noise/WP-1304

Page, J.A. and K.J. Plotkin, (2004) *Acoustic Repropagation Technique, Version 3 (ART3)*, Wyle Research Report, WR 03-25, Wyle Laboratories, Inc., Arlington, VA. April.

George A.R. and S-T Chou, (1984) *Comparison of Broadband Noise Mechanisms, Analyses, and Experiments on Rotors*, Vol. 21, No. 8, Jrnl Aircraft, August.